A novel non-invasive method to sample immune cells in the lower female genital tract[1]

Authors: M. Quinn Peters[1], Eva Domenjo-Vila[2], Marc Carlson[3], Paul T. Edlefsen[4], Melanie Gasper[1], Smritee Dabee[1], Blair Armistead[1], Christopher Whidbey[5], Heather B. Jaspan[1,6,7], Martin Prlic[2,7], Whitney E. Harrington[1,6,7*]

Affiliations:

[1]Center for Global Infectious Disease Research, Seattle Children's Research Institute; Seattle, WA, USA

[2]Vaccine and Infectious Disease Division, Fred Hutchinson Cancer Research Center; Seattle, WA, USA

[3]Research Scientific Computing, Enterprise Analytics, Seattle Children's Research Institute; Seattle, WA, USA

[4]Statistical Center for HIV/AIDS Research and Prevention, Vaccine and Infectious Disease Division, Fred Hutchinson Cancer Research Center, Seattle, Washington, USA

[5]Department of Chemistry, Seattle University; Seattle, WA, USA

[6]Department of Pediatrics, University of Washington; Seattle, WA, USA

[7]Department of Global Health, University of Washington; Seattle, WA, USA

*Corresponding Author. Email: whitney.harrington@seattlechildrens.org

[1] Institute of Translational Health Sciences, University of Washington 415600010101

University of Washington and Seattle Children's Research Institute Seed Funds

ABSTRACT

T cells in the female genital tract (FGT) are a key mediator of susceptibility to and protection from infection, including HIV and other sexually transmitted infections. There is a critical need for increased understanding of the distribution and activation of T cell populations in the FGT, but current sampling methods are invasive and expensive, limiting the ability to study these populations longitudinally. To address these challenges, we have developed a novel method to sample immune cells from the FGT utilizing disposable menstrual discs which are non-invasive, self-applied, and low-cost. To demonstrate reproducibility, we sampled the cervicovaginal fluid (CVF) of healthy, reproductive-aged individuals using menstrual discs over three sequential days. CVF was processed for cervicovaginal cells, and high parameter flow cytometry was used to characterize immune populations. We identified large numbers of live, CD45+ leukocytes, as well as populations of T cells and B cells. Within the T cell compartment, phenotypic features of T cell subsets were consistent with previous FGT studies utilizing more invasive approaches, including identification of both tissue resident and migratory populations. In addition, the T cell population structure was highly reproducible across days within individuals but divergent across individuals. Our novel approach to sampling immune cells in the FGT will decrease barriers to participation and empower longitudinal sampling in future research studies.

INTRODUCTION

In the female genital tract (FGT), the ectocervix and vagina are the primary sites of exposure to HIV and other sexually transmitted infections (STI) [1, 2]. Local T cells at these sites are key mediators of both susceptibility to and protection from infection [3]. For example, non-specific inflammation may lead to T cell activation and increased risk of HIV acquisition [2, 4-7]. In contrast, robust Th1 responses are needed for clearance of pathogens such as *Chlamydia trachomatis* [8]. In addition, T cells patrolling the FGT must tolerate resident microbes and other foreign antigens such as those from semen [5, 9-11]. Prior phenotypic and transcriptional profiling of mucosal T cell populations has demonstrated that they are highly adapted to their site of residence and distinct from those in circulation, emphasizing the critical need to sample these populations directly from the site of interest [12-14]. For example, within the FGT limited work describes an association between cervical T cell populations, menstrual cycle, and microbial community state; however, these studies have been limited by small sample sizes [15-17]. Despite the intriguing associations between the FGT and these biological variables, it has been challenging to comprehensively characterize their complex interplay in diverse populations due to the difficulty in sampling the FGT longitudinally.

Common methods for sampling immune cell populations in the FGT include biopsy, cytobrush, and cervicovaginal lavage (CVL) [18, 19]. Tissue collected either from biopsy or discarded surgical tissue is considered the “gold standard” in the field for obtaining large cell yields and allows for precise sampling of anatomical sites [18, 19]. This approach has identified two key T cell populations in the FGT: tissue resident memory (T_{RM}) cells and migratory cells, which circulate between the tissue, regional lymph nodes, and peripheral blood [17, 20, 21]. However, these important studies were limited by small sample sizes, and most were conducted at a single time point. Cytobrushes have been used to elucidate endocervical CD4+ and CD8+ T cell populations including the impact of HIV [22-25], but the collection

site is anatomically distinct from ectocervical biopsy and may preferentially sample monocytes over lymphocytes [18, 26, 27]. In addition, both biopsy and cytobrush may disrupt the mucosal barrier and temporarily increase susceptibility to or transmission of infection, including HIV [28]. CVL, in contrast, collects T cells present in the cervical fornixes and vaginal lumen (i.e., "luminal" T cells), and does not disrupt the mucosal barrier of the FGT. However, CVL yields substantially fewer cells than cytobrush and tissue biopsy sampling [18]. Finally, each of these methods requires implementation by a health care provider in a clinical setting with a speculum exam, which can be both uncomfortable and expensive, limiting number of participants and time points for longitudinal sampling.

Here, we present a novel, non-invasive approach to sample luminal T cells from the FGT, utilizing self-inserted menstrual discs to collect cervicovaginal fluid (CVF). Menstrual discs are a disposable product designed to collect menstrual fluid. In addition, they can be used to collect CVF in individuals while not menstruating [29, 30] (**Figure 1A, B**). We have found that this approach yields high numbers of immune cells including T cells and captures both tissue resident and migratory populations with reproducible distributions and phenotypic features within individuals. This inexpensive, non-invasive approach reduces barriers associated with sequential sampling and empowers a larger and more diverse population of individuals, particularly those with limited access to clinical and research settings, to participate in future studies of FGT immunity.

MATERIALS AND METHODS

Cohort

All participants were enrolled into the Center for Global Infectious Disease Research Biorepository, approved by the Seattle Children's Research Institute Institutional Review Board (STUDY00002048). Participants self-reported as healthy, not pregnant, reproductive age, weighing > 110 pounds, and none

had an intrauterine device or a known hormonal disorder. To validate the reproducibility of our protocol, five participants were invited to donate CVF samples on three sequential days, 7-11 from last menstrual period (LMP) during the follicular phase, as well as one blood sample. One participant (participant 3) did not menstruate due to oral contraceptive use, so timing was not relative to LMP. Information on acute and chronic medical conditions and medication usage was also collected.

Sample Collection

Whole blood was drawn into ethylenediaminetetraacetic acid (EDTA) vacutainer tubes (BD Biosciences). Blood was processed for peripheral blood mononuclear cells (PBMCs) as previously described [31]. For CVF collection, Softdisc® menstrual discs were self-inserted by participants and worn for up to 4 hours. After self-retrieval, menstrual discs were placed in a 50 mL conical tube and returned to the study team. CVF was stored at 4˚C until processing.

Protocol for Processing of CVF From Menstrual Discs

Discs were initially processed in 50 mL conical tubes returned by participants (**Figure 1C**). Discs were submerged in 10 mL of complete RPMI (RPMI with L-glutamine, 10% fetal bovine serum (FBS), 100 U/ml penicillin, 100 µg/ml streptomycin) and rinsed 5 times in the medium using a serological pipet to dislodge CVF. The tube containing the disc was centrifuged at 250 x *g* for 7 minutes at 4°C. The menstrual disc was then removed from the tube using sterile forceps and remaining CVF was transferred from the disc to the tube by pipet. The catch tray of the menstrual disc was rinsed with 1 mL of sterile PBS with 2% FBS (FACS buffer), which was transferred to the tube, and the disc was discarded. Mucins were degraded by incubating CVF with 1 mM dithiothreitol (DTT) for 30 minutes in a 37°C incubator with 5% CO_2, as described [32]. The solution was then filtered through a 100 µm nylon cell strainer (VWR) and centrifuged at 400 x *g* for 10 minutes at 4°C and the supernatant was discarded. The resulting cell pellet

of cervicovaginal cells (CVC) was washed twice with 40 mL sterile PBS with 2% FBS, and cells were enumerated using a C-Chip hemocytometer (INCYTO). For cryopreservation, the cell pellet was resuspended in 1 mL freezing medium (50% FBS, 40% RPMI with L-glutamine, 10% DMSO (Millipore Sigma)), transferred to a cryovial, placed in a 1°C cryogenic freezing container at -80°C overnight, and then transferred to liquid nitrogen.

Prior to flow cytometric analysis, CVC and PBMC were thawed in a 37°C water bath, transferred to pre-warmed thaw medium (RPMI with L-glutamine, 20% FBS), and centrifuged at 400 x *g* for 5 minutes. Cell pellets were resuspended in 2 mL cRPMI and enumerated. CVF was enriched for CD45+ cells using the EasySep™ Release Human CD45 Positive Selection Kit (Stem Cell Technologies) according to manufacturer protocol. The resulting CD45 depleted fraction underwent a second enrichment to recover any remaining CD45+ cells, and the two CD45-enriched fractions were combined.

Cell staining and flow cytometry acquisition

All flow cytometry was performed at Fred Hutchison Cancer Center utilizing a 28-color panel focused on T cell phenotyping (**Supplementary Table 1**) [33]. CVC and PBMC were incubated with Fc-blocking reagent (BioLegend) and fixable UV Blue Live/Dead reagent (ThermoFisher) in PBS for 15 minutes at room temperature. Cells were then stained with 50 µL of extracellular antibody master mix in Brilliant Stain Buffer (BD Bioscience) for 20 minutes at room temperature. Stained cells were washed and resuspended in FACS buffer. For intracellular and intranuclear staining, the cells were fixed with freshly prepared fixation buffer (ThermoFisher) for 30 minutes at room temperature, washed, and then stained with 50 µL of intracellular antibody master mix in FACS buffer for 20 minutes at room temperature. Cells were then washed and resuspended in FACS buffer and kept at 4°C protected from light until analysis. Single-stained compensation controls were prepared for each experiment using antibody capture beads

(BD Biosciences) diluted in FACS buffer and amine reactive beads (ArC™ Amine Reactive Compensation Bead Kit, Themo Fisher). Data was acquired using a FACSymphony A5 (BD Biosciences) and FACSDiva acquisition software (BD Biosciences). All samples were run in the same experiment to eliminate batch effects.

Flow cytometry analysis

Flow cytometry data were analyzed using FlowJo v10.8 software (FlowJo, LLC). The pre-determined gating scheme was applied uniformly across all samples. Initial panel development included fluorescence minus one to set gates [33]. A technical replicate sample that had been validated in prior experiments with the same panel and instrument was included to inform gating. Briefly, paired CVC and PBMC were gated on CD45+ and viability, then CD3+ and CD19+ populations (**Figure 2A**). After gating out MAIT and γδ-T cells, CD3+ T cells were gated into CD4+ and CD8+ T cell populations. Within the CD4+ T cell population, regulatory T cells (Tregs) were designated as CD25+/CD127-, and the remaining cells were designated as conventional CD4+ cells. CD8+, CD4+, and Treg populations were then gated for memory, tissue residency, activation, and suppression markers. Phenotypic analysis was restricted to samples where the parent population of interest contained >=50 T cells. Cell count, frequency, and mean fluorescence intensity (MFI) were determined in FlowJo.

Integrated high-parameter data analysis was restricted to CVC samples containing >=100 T cells. Comparison of global T cell population structure across samples was first conducted in R v4.3.2 using Principal Component Analysis (PCA) computed from MFI of phenotypic markers relevant to viable conventional T cells (i.e., live/dead, CD45, CD19, MR1-tet, and γδ-TCR were excluded). PCA plots were visualized using ggplot2 [34]. Initial comparison included both CVC and PBMC, where only memory T cell populations were considered (i.e., naïve T cells excluded), as well as subsequent analysis considering

only CVC. Comparison of local T cell population structure across all samples was performed using FlowSOM and ConsensusClusterPlus in the integrated CATALYST R package [35]. For data preparation, the compensation matrix and gating scheme used for FlowJo analyses was applied to raw flow cytometry data in R using flowCore and CytoML [36, 37]. T cells across CVC samples were clustered using median fluorescent intensity of the T cell-directed markers used in PCA with a maximum metacluster number of 20. The number of clusters examined for subsequent analysis (k=12) was determined by cluster stability measure when the relative change in area under a Cumulative Distribution Function curve approached zero. The aggregated marker expression within T cell clusters was scaled from 0 to 1 and visualized with a heatmap; hierarchical clustering is shown with dendrograms representing Euclidean distance and plotted with average linkage. Relative abundances of the clusters in each CVC sample were plotted to demonstrate reproducibility in population structure within individuals across samples. Fluorescent intensity data for each cell was dimensionally reduced and visualized using uniform manifold approximation and projection (UMAP) without the default CATALYST data transformation. The resulting UMAP was colored by FlowSOM assigned clusters.

Statistical Analysis

Cell count data (e.g., number of CD3+ T cells recovered) are presented as medians. Frequencies of parent populations (e.g., % Tregs of CD4+ T cells) are presented as means. To compare frequency of populations between CVC and PBMC, a mean frequency of the CVC population across all sampled days was computed. The mean frequency of the population in the CVC was then compared with the frequency in paired PBMC. Given the small sample size and paired data structure, p values were computed with a Wilcoxon signed rank test. Significance was defined as a p value less than or equal to 0.05. Analysis was conducted in Stata 14.2.

RESULTS

Overview of Immune Cells Recovered from CVF

Total number of viable CD45+ cells recovered from CVF samples varied both between and within individuals (**Supplementary Table 2**). The median number of viable CD45+ cells recovered from CVF was 6,235. Within the CD45+ cell population, CD3+ T cells were the largest subpopulation (median = 1,182 cells), but there was also high recovery of CD19+ B cells (median = 1,072) (**Table 1**). Of CD3+ T cells, frequencies ranged from 37-87% for CD4+ T cells and 7-55% for CD8+ T cells. The majority of CVC T cells were antigen-experienced (mean: 97% of conventional CD4+ cells and 91% of CD8+ cells), including central memory (CCR7+ CD45RA-), effector memory (CCR7- CD45RA-), and terminally differentiated effector RA+ populations (CCR7-, CD45RA+) **(Figure 2B-E)**. The CD8+ compartment of CVC contained both T_{RM} (CD69+ CD103+) (**Figure 2F**) and migratory populations, and CD8+ T_{RM} were significantly enriched in CVMC relative to PBMC (mean: 15% vs. 0.03%, p=0.04). In addition to CCR7+ and CCR7- conventional populations, CVC CD4+ T cells also contained a Treg population (**Figure 2G**), the frequency of which was enriched compared to PBMC (mean: 14% vs 4%, p=0.04). Similar to conventional CD4+ T cells, 98% of Tregs were antigen experienced. Within CVC CD4 T cells, the expression of PD-1 and CCR5 was highest on Tregs, relative to conventional CD4+ T cells, and was consistent across sampling days within individuals (**Figure 2 H-I**).

Activation and Suppression Phenotype of CVC T cells

We next compared the activation and suppression phenotype of specific FGT T cell populations of interest reported in prior studies, specifically CD4+ T regs and memory CD8+ T cells [20, 38]. Relative to PBMC, a higher frequency of CVC CD4+ Tregs expressed the activation marker CCR5 (mean: 77% vs. 39%, p=0.04) and the suppressive markers ICOS (mean: 54% vs 21%, p=0.04), PD-1 (mean: 47% vs 5%, p=0.04), LAG-3 (mean: 30% vs. 4%, p=0.04), CTLA-4 (mean: 38% vs. 7%, p=0.04), and TIM-3 (mean:

42% vs. 4%, p=0.04) (**Figure 3A, B**). The Treg compartment also contained populations of PD-1+ TIM3+ cells (10 to 45% within samples), a highly suppressive phenotype observed in tissue Treg populations and rarely observed in the periphery [39]. Within CVC memory CD8+ T cells there was a higher frequency of cells expressing CCR5 (mean: 85% vs. 25%, p=0.04), HLA-DR (activation) (mean: 40% vs 11%, p=0.04), and PD-1 (mean: 4% vs. 7%, p=0.04) relative to PBMC (**Figure 3C, D**). Although the frequencies of memory CD8+ T cells expressing CD38 (mean: 23% vs 11%, p=0.08) and granzyme B (mean: 32% vs. 25%, p=0.7) was higher in CVC versus PBMC, these differences did not reach significance. Together these observations indicate that menstrual disc sampling yielded populations of T cells consistent with those previously described using more invasive sampling methods.

Reproducibility of T cell Population Structure

To quantify the reproducibility of global CVC T cell population structure across sequential timepoints within individuals, we compared memory T cell phenotypes across consecutive days from the FGT, as well as paired PBMC from one timepoint, using PCA. When comparing CVC and PBMC memory T cell populations, samples clustered clearly by sample type (**Figure 4A**). Within CVC CD3+ and CD4+ T cell populations, by comparison, samples clustered by individual (**Figure 4B, C**). There was no clear relationship between day of sampling and clustering pattern for any analysis. Within CD3+ populations, the largest contributors to PC1 as determined by loading scores were CD4, activation markers (CD28 and CD38), and suppressive markers (PD-1, CTLA-4, ICOS, and TIM3); the largest contributors to PC2 were memory markers (CD45RA, CCR7, and CD27) and the proliferation marker KI67. Within the CD4+ population, the largest contributors to PC1 were activation markers (CCR5, CD69, CD38, and CD28) and suppressive markers (PD-1, CTLA-4, and TIM3); the largest contributors to PC2 were also activation (HLA-DR, CD137, CD25) and suppressive markers (PD-1, LAG3). Together these observations

emphasize that individuals have unique patterns of memory, activation, and suppression markers on CVC T cells that are highly conserved across days.

We next examined local CVC T cell population structure across participants using the CATALYST tool. Consistent with our PCA analysis, initial analysis looking at marker expression demonstrated two groups of participants separated by degree of T cell activation (e.g., CCR5 expression was high in participant 1, 3, and 5 and low in participant 2 and 4) (**Figure 4D**). We next clustered T cells across all individuals to understand shared population structure. Across all participants, luminal T cells were comprised of two large populations (CD4+ and CD8+) and a distinct minor population, which could be subdivided into 12 phenotypic clusters (**Figure 4E, F**). Clusters 4, 5, 6, 7, 11, and 12 had high expression of CD4; clusters 1, 2, and 3 had high expression of CD8; and clusters 8, 9, and 10 were both CD4 and CD8 low. The predominant CD4 cluster (cluster 5) demonstrated low CCR7, CD45RA, CD69, and CD103 expression and moderate activation (CCR5) consistent with an effector memory-like population. Within the additional CD4 dominant clusters, there was variable expression of activation and suppressive markers. Within the CD8 clusters, clusters 1 and 3 were consistent with T_{RM} populations which differed by degree of effector capacity (e.g., granzyme B), whereas cluster 2 was consistent with a naïve-like population (CCR7 and CD45RA high). Clusters 8, 9, and 10 had lower expression of CD3 and CD4 and were CD8 negative but had high expression of granzyme B, CD137, and HLA-DR, and expression of CD161 in cluster 9, possibly consistent with NKT cells. Within individuals, the proportion of each cluster was recapitulated across timepoints (**Figure 4G**). Together these observations indicate that luminal T cells from the FGT are comprised of diverse populations which vary by tissue residence, activation, and suppressive status and that the distribution of these populations within individuals is preserved across sequential days.

DISCUSSION

The cervix is a critical site for exposure and acquisition of HIV and other STIs. It is thus essential to understand the immune cell populations at this site, as well as how these populations vary longitudinally and in response to variables such as hormonal fluctuations, microbial communities, hygiene practices, and sexual behaviors. Here, we describe a novel, non-invasive method for obtaining large numbers of live CD45+ immune cells from CVF using menstrual discs. These samples are rich in T cells and an abundant source of B cells and HLA-DR+ populations, which remain viable after cryopreservation.

To compare our FGT sampling method to those reported in the literature, we conducted in depth phenotyping of the T cell populations. We identified FGT T cell populations that closely resembled those previously identified in biopsy and surgically resected tissue, including both migratory and tissue resident populations [38]. Consistent with prior reports, both conventional CD4 and CD8 populations had high expression of CCR5, indicating activation, and for CD4+ cells representing an HIV target cell population [17, 20]. In addition, Tregs were enriched and showed high expression of suppressive markers [38]. Similarly, we identified CD8+ T_{RM}, although the overall frequency was lower relative to those reported from biopsy [13, 20, 21]. These data indicate that our sampling approach identifies key T cell subsets consistent with prior invasive approaches.

Importantly, our sampling method collects luminal T cells, similar to prior work utilizing CVL. In addition to representing the underlying tissue, data from lung suggest that luminal T cells may contain unique populations, which have discrete function via their ability to migrate between the lumen and the tissue [40-42]. More recently, studies using CVL in non-human primates have identified a unique population of memory CD4+ T cells that migrate into the lumen of the FGT in a CCR5-dependent manner [17]. In the

context of the cervicovagina, luminal T cells may preferentially encounter bacteria present as part of vaginal microbiota versus pathogenic bacteria and viruses, which invade the tissue. In this light, independent study of luminal T cells, not merely as a representation of tissue, may yield novel insights into the immunology of the cervicovagina.

Intra-individual reproducibility is critical for any sampling method, so we assessed the reproducibility of our approach across three sequential days. Despite variability in absolute viable leukocyte recovery, the T cell population structure was maintained within each individual. Within individuals, we identified high reproducibility of both the global local population structure, including the distribution of CVC T cell populations and specific phenotypic characteristics (e.g., the expression of PD-1 on conventional CD4+ T cells). In contrast, we observed significant inter-individual variability, wherein each participant had a unique T cell population structure which was reproducible across time. These observations suggests that differences observed across individuals may be driven by biological or behavioral variability. This highlights the need for further study to evaluate the role of specific factors in driving CVC T cell population structure across individuals.

Our study has a number of limitations. For example, the absolute number of leukocytes collected each day varied across replicates. This may reflect differences in cervical secretions day to day, variable positioning of the disc, or changes in activity level. Despite this variation, the relative population structure was preserved. In addition, different sampling methods will sample different anatomical zones and yield different populations. The high CD4:CD8 cell ratio of our CVC T cells is most consistent with cervical origin [21], but it should be noted that CVF collected via menstrual disc contains cells which are of less precise anatomical origin than endocervical cytobrush or tissue biopsy. Our flow cytometry panel was

primarily targeted at T cell phenotyping, so we were not able to assess the relative lymphocyte to monocyte frequency; however, we did identify a large population of CD3- CD19- HLA-DR+ cells that fell within the expected forward and side scatter of monocytes. Finally, participants may be unfamiliar with the use of menstrual discs, with a risk of incorrect placement in the vagina rather than surrounding the cervix. To address this in future studies, study team members could demonstrate correct positioning of the disc prior to utilization.

We have established a novel method for cervicovaginal sampling that is low cost, non-invasive, and self-administered. This method can be used in longitudinal studies and does not require study participants to interact with a health care provider or a clinical setting, reducing the barrier to participation. The high population reproducibility, low cost, and ability to cryopreserve these samples with sufficient cell recovery further emphasizes the potential application of this approach in future studies, such as in large scale vaccine trials that may take place at multiple sites.

Acknowledgements

We thank the study participants who donated blood and CVF.

REFERENCES

1.Van Gerwen OT, Muzny CA, and M. JM, *Sexually transmitted infections and female reproductive health.* Nat Microbiol, 2022. **7**(8): p. 1116-1126.

2.Yi TJ, Shannon B, Prodger J, McKinnon L, and K. R, *Genital immunology and HIV susceptibility in young women.* Am J Reprod Immunol, 2013. **69**: p. 74-79.

3.Soghoian DZ, Jessen H, Flanders M, Sierra-Davidson K, Cutler S, Pertel T, Ranasinghe S, Lindqvist M, Davis I, Lane K, Rychert J, Rosenberg ES, Piechocka-Trocha A, Brass AL, Brenchley JM, Walker BD, and S. H, *HIV-specific cytolytic CD4 T cell responses during acute HIV infection predict disease outcome.* Sci Transl Med, 2012. **4**(123).

4.Dabee, S., S.L. Barnabas, K.S. Lennard, S.Z. Jaumdally, H. Gamieldien, C. Balle, A.U. Happel, B.D. Murugan, A.L. Williamson, N. Mkhize, J. Dietrich, D.A. Lewis, F. Chiodi, T.J. Hope, R. Shattock, G. Gray, L.G. Bekker, H.B. Jaspan, and J.S. Passmore, *Defining characteristics of genital health in South African adolescent girls and young women at high risk for HIV infection.* PLoS One, 2019. **14**(4): p. e0213975.

5.Jewanraj, J., S. Ngcapu, F. Osman, V. Ramsuran, M. Fish, A. Mtshali, R. Singh, L.E. Mansoor, S.S. Abdool Karim, Q. Abdool Karim, J.S. Passmore, and L.J.P. Liebenberg, *Transient association between semen exposure and biomarkers of genital inflammation in South African women at risk of HIV infection.* J Int AIDS Soc, 2021. **24**(6): p. e25766.

6.Masson, L., J.A. Passmore, L.J. Liebenberg, L. Werner, C. Baxter, K.B. Arnold, C. Williamson, F. Little, L.E. Mansoor, V. Naranbhai, D.A. Lauffenburger, K. Ronacher, G. Walzl, N.J. Garrett, B.L. Williams, M. Couto-Rodriguez, M. Hornig, W.I. Lipkin, A. Grobler, Q. Abdool Karim, and S.S. Abdool Karim, *Genital inflammation and the risk of HIV acquisition in women.* Clin Infect Dis, 2015. **61**(2): p. 260-9.

7.Arnold, K.B., A. Burgener, K. Birse, L. Romas, L.J. Dunphy, K. Shahabi, M. Abou, G.R. Westmacott, S. McCorrister, J. Kwatampora, B. Nyanga, J. Kimani, L. Masson, L.J. Liebenberg, S.S. Abdool Karim, J.A. Passmore, D.A. Lauffenburger, R. Kaul, and L.R. McKinnon, *Increased levels of inflammatory cytokines in the female reproductive tract are associated with altered expression of proteases, mucosal barrier proteins, and an influx of HIV-susceptible target cells.* Mucosal Immunol, 2016. **9**(1): p. 194-205.

8.Labuda, J.C., O.H. Pham, C.E. Depew, K.D. Fong, B.S. Lee, J.A. Rixon, and S.J. McSorley, *Circulating immunity protects the female reproductive tract from Chlamydia infection.* Proc Natl Acad Sci U S A, 2021. **118**(21).

9.Ravel J, Gajer P, Abdo Z, Schneider GM, Koenig SS, McCulle SL, Karlebach S, Gorle R, Russell J, Tacket CO, Brotman RM, Davis CC, Ault K, Peralta L, and F. LJ, *Vaginal microbiome of reproductive-age women.* PNAS, 2011. **108**: p. 4680-4687.

10.Campisciano G, Zanotta N, Licastro D, De Seta F, and C. M, *In vivo microbiome and associated immune markers: New insights into the pathogenesis of vaginal dysbiosis.* Scientific Reports, 2018. **8**(1): p. 2307.

11.De Seta, F., G. Campisciano, N. Zanotta, G. Ricci, and M. Comar, *The Vaginal Community State Types Microbiome-Immune Network as Key Factor for Bacterial Vaginosis and Aerobic Vaginitis.* Front Microbiol, 2019. **10**: p. 2451.

12.Poon MML, Caron DP, Wang Z, Wells SB, Chen D, Meng W, Szabo PA, Lam N, Kubota M, Matsumoto R, Rahman A, Luning Prak ET, Shen Y, Sims PA, and F. DL, *Tissue adaptation and clonal segregation of human memory T cells in barrier sites.* Nat Immunol, 2023. **24**(2): p. 309-319.

13.Davé VA, Cardozo-Ojeda EF, Mair F, Erickson J, K.A. Woodward-Davis AS, Soerens A, Czartoski J, Teague C, Potchen N, Oberle S, Zehn D, Schiffer JT, Lund JM, and P. M, *Cervicovaginal Tissue*

Residence Confers a Distinct Differentiation Program upon Memory CD8 T Cells. J Immunol, 2021. **206**(12): p. 2937-2948.

14.Kumar, B.V., W. Ma, M. Miron, T. Granot, R.S. Guyer, D.J. Carpenter, T. Senda, X. Sun, S.H. Ho, H. Lerner, A.L. Friedman, Y. Shen, and D.L. Farber, *Human Tissue-Resident Memory T Cells Are Defined by Core Transcriptional and Functional Signatures in Lymphoid and Mucosal Sites.* Cell Rep, 2017. **20**(12): p. 2921-2934.

15.Gosmann C, Anahtar MN, Handley SA, Farcasanu M, Abu-Ali G, Bowman BA, Padavattan N, Desai C, Droit L, Moodley A, Dong M, Chen Y, Ismail N, Ndung'u T, W.D. Ghebremichael MS, Mitchell C, Dong KL, Huttenhower C, Walker BD, Virgin HW, and K. DS, *Lactobacillus-Deficient Cervicovaginal Bacterial Communities are Associated with Increased HIV Acquisition in Young South African Women.* Immunity, 2017. **46**(1): p. 29-37.

16.Anahtar MN, Byrne EH, Doherty KE, Bowman BA, Yamamoto HS, Soumillon M, Padavattan N, M.A. Ismail N, Sabatini ME, N.C. Ghebremichael MS, Huttenhower C, Virgin HW, Ndung'u T, Dong KL, Walker BD, Fichorova RN, and K. DS, *Cervicovaginal bacteria are a major modulator of host inflammatory responses in the female genital tract.* Immunity, 2015. **42**(5): p. 965-967.

17.Swaims-Kohlmeier, A., R.E. Haaland, L.B. Haddad, A.N. Sheth, T. Evans-Strickfaden, L.D. Lupo, S. Cordes, A.J. Aguirre, K.A. Lupoli, C.Y. Chen, I. Ofotukun, C.E. Hart, and J.E. Kohlmeier, *Progesterone Levels Associate with a Novel Population of CCR5+CD38+ CD4 T Cells Resident in the Genital Mucosa with Lymphoid Trafficking Potential.* J Immunol, 2016. **197**(1): p. 368-76.

18.McKinnon LR, Hughes SM, De Rosa SC, Martinson JA, Plants J, Brady KE, Gumbi PP, Adams DJ, Vojtech L, Galloway CG, Fialkow M, Lentz G, Gao D, Shu Z, Nyanga B, Izulla P, Kimani J, Kimwaki S, Bere A, Moodie Z, Landay AL, Passmore JA, Kaul R, Novak RM, McElrath MJ, and H. F, *Optimizing viable leukocyte sampling from the female genital tract for clinical trials: an international multi-site study.* PLoS One, 2014. **9**(1).

19.Lund, J.M., F. Hladik, and M. Prlic, *Advances and challenges in studying the tissue-resident T cell compartment in the human female reproductive tract.* Immunol Rev, 2023. **316**(1): p. 52-62.

20.Pattacini L, Woodward Davis A, Czartoski J, Mair F, Presnell S, Hughes SM, Hyrien O, Lentz GM, Kirby AC, Fialkow MF, Hladik F, Prlic M, and L. JM, *A pro-inflammatory CD8+ T-cell subset patrols the cervicovaginal tract.* Mucosal Immunol, 2019. **12**(5): p. 1118-1129.

21.Woodward Davis, A.S., S.C. Vick, L. Pattacini, V. Voillet, S.M. Hughes, G.M. Lentz, A.C. Kirby, M.F. Fialkow, R. Gottardo, F. Hladik, J.M. Lund, and M. Prlic, *The human memory T cell compartment changes across tissues of the female reproductive tract.* Mucosal Immunol, 2021. **14**(4): p. 862-872.

22.Liebenberg, L.J., H. Gamieldien, N.N. Mkhize, S.Z. Jaumdally, P.P. Gumbi, L. Denny, and J.A. Passmore, *Stability and transport of cervical cytobrushes for isolation of mononuclear cells from the female genital tract.* J Immunol Methods, 2011. **367**(1-2): p. 47-55.

23.Iqbal, S.M., T.B. Ball, J. Kimani, P. Kiama, P. Thottingal, J.E. Embree, K.R. Fowke, and F.A. Plummer, *Elevated T cell counts and RANTES expression in the genital mucosa of HIV-1-resistant Kenyan commercial sex workers.* J Infect Dis, 2005. **192**(5): p. 728-38.

24.Horton, R.E., N. Kaefer, E. Songok, F.B. Guijon, N. Kettaf, G. Boucher, R.P. Sekaly, T.B. Ball, and F.A. Plummer, *A comparative analysis of gene expression patterns and cell phenotypes between cervical and peripheral blood mononuclear cells.* PLoS One, 2009. **4**(12): p. e8293.

25.Rebbapragada, A., K. Howe, C. Wachihi, C. Pettengell, S. Sunderji, S. Huibner, T.B. Ball, F.A. Plummer, W. Jaoko, and R. Kaul, *Bacterial vaginosis in HIV-infected women induces reversible alterations in the cervical immune environment.* J Acquir Immune Defic Syndr, 2008. **49**(5): p. 520-2.

26.Juno, J.A., G. Boily-Larouche, J. Lajoie, and K.R. Fowke, *Collection, isolation, and flow cytometric analysis of human endocervical samples.* J Vis Exp, 2014(89).

27.Hirbod, T., J. Kimani, A. Tjernlund, J. Cheruiyot, A. Petrova, T.B. Ball, N. Mugo, W. Jaoko, F.A. Plummer, R. Kaul, and K. Broliden, *Stable CD4 expression and local immune activation in the ectocervical mucosa of HIV-infected women.* J Immunol, 2013. **191**(7): p. 3948-54.

28.Woo, V.G., T. Liegler, C.R. Cohen, G.F. Sawaya, K. Smith-McCune, E.A. Bukusi, and M.J. Huchko, *Association of cervical biopsy with HIV type 1 genital shedding among women on highly active antiretroviral therapy.* AIDS Res Hum Retroviruses, 2013. **29**(7): p. 1000-5.

29.Jenkins, D.J., B.M. Woolston, M.I. Hood-Pishchany, P. Pelayo, A.N. Konopaski, M. Quinn Peters, M.T. France, J. Ravel, C.M. Mitchell, S. Rakoff-Nahoum, C. Whidbey, and E.P. Balskus, *Bacterial amylases enable glycogen degradation by the vaginal microbiome.* Nat Microbiol, 2023. **8**(9): p. 1641-1652.

30.Nunn, K.L., G.C. Clair, J.N. Adkins, K. Engbrecht, T. Fillmore, and L.J. Forney, *Amylases in the Human Vagina.* mSphere, 2020. **5**(6).

31.Armistead B, Jiang Y, Carlson M, Ford ES, Jani S, Houck J, Wu X, Jing L, Pecor T, Kachikis A, Yeung W, Nguyen T, Coig R, Minkah N, Larsen SE, Coler RN, Koelle DM, and H. WE, *Spike-specific T cells are enriched in breastmilk following SARS-CoV-2 mRNA vaccination.* Mucosal Immunol, 2023. **16**(1): p. 39-49.

32.Chiodini, R.J., S.E. Dowd, W.M. Chamberlin, S. Galandiuk, B. Davis, and A. Glassing, *Microbial Population Differentials between Mucosal and Submucosal Intestinal Tissues in Advanced Crohn's Disease of the Ileum.* PLoS One, 2015. **10**(7): p. e0134382.

33.Mair, F., J.R. Erickson, M. Frutoso, A.J. Konecny, E. Greene, V. Voillet, N.J. Maurice, A. Rongvaux, D. Dixon, B. Barber, R. Gottardo, and M. Prlic, *Extricating human tumour immune alterations from tissue inflammation.* Nature, 2022. **605**(7911): p. 728-735.

34.Wickham, H., *ggplot2: Elegant Graphics for Data Analysis*. 2016: Springer-Verlag New York.

35.Crowell H, Z.V., Chevrier S, Robinson M, *CATALYST: Cytometry dATa anALYSis Tools.* 2023: Bioconductor.

36.Hahne, F., N. LeMeur, R.R. Brinkman, B. Ellis, P. Haaland, D. Sarkar, J. Spidlen, E. Strain, and R. Gentleman, *flowCore: a Bioconductor package for high throughput flow cytometry.* BMC Bioinformatics, 2009. **10**: p. 106.

37.Finak, G., W. Jiang, and R. Gottardo, *CytoML for cross-platform cytometry data sharing.* Cytometry A, 2018. **93**(12): p. 1189-1196.

38.Traxinger, B., S.C. Vick, A. Woodward-Davis, V. Voillet, J.R. Erickson, J. Czartoski, C. Teague, M. Prlic, and J.M. Lund, *Mucosal viral infection induces a regulatory T cell activation phenotype distinct from tissue residency in mouse and human tissues.* Mucosal Immunol, 2022. **15**(5): p. 1012-1027.

39.Sakuishi, K., S.F. Ngiow, J.M. Sullivan, M.W. Teng, V.K. Kuchroo, M.J. Smyth, and A.C. Anderson, *TIM3(+)FOXP3(+) regulatory T cells are tissue-specific promoters of T-cell dysfunction in cancer.* Oncoimmunology, 2013. **2**(4): p. e23849.

40.Kohlmeier, J.E., S.C. Miller, and D.L. Woodland, *Cutting edge: Antigen is not required for the activation and maintenance of virus-specific memory CD8+ T cells in the lung airways.* J Immunol, 2007. **178**(8): p. 4721-5.

41.McMaster, S.R., J.J. Wilson, H. Wang, and J.E. Kohlmeier, *Airway-Resident Memory CD8 T Cells Provide Antigen-Specific Protection against Respiratory Virus Challenge through Rapid IFN-gamma Production.* J Immunol, 2015. **195**(1): p. 203-9.

42.Horvath, C.N., C.R. Shaler, M. Jeyanathan, A. Zganiacz, and Z. Xing, *Mechanisms of delayed anti-tuberculosis protection in the lung of parenteral BCG-vaccinated hosts: a critical role of airway luminal T cells.* Mucosal Immunol, 2012. **5**(4): p. 420-31.

Author Contributions

Methodology: MQP, EDV, MC, PTE, MG, SD, HBJ, MP, CW, WEH

Participant enrollment: MQP, WEH

Investigation: MQP, WEH

Visualization: MQP, MC, BA, WEH

Formal Analysis: MQP, MC, PTE, SD, WEH

Funding Acquisition: MQP, BA, WEH

Supervision: MP, WEH

Writing—Draft Preparation: MQP, WEH

Writing—Review and Editing: MQP, EDV, MC, PTE, MG, SD, HBJ, MP, CW, WEH

Competing interests: The authors have no completing interests.

Table 1. Counts of immune cell populations across CVF samples

Cell type	Median cells (range)
CD45+	6,233 (212-57,703)
CD3+	1,182 (12-11,554)
CD4+	938 (5-7,484)
CD8+	163 (2-3,404)
CD19+	1,072 (8-4,690)
CD3- CD19- HLA-DR+	775 (32-12,849)

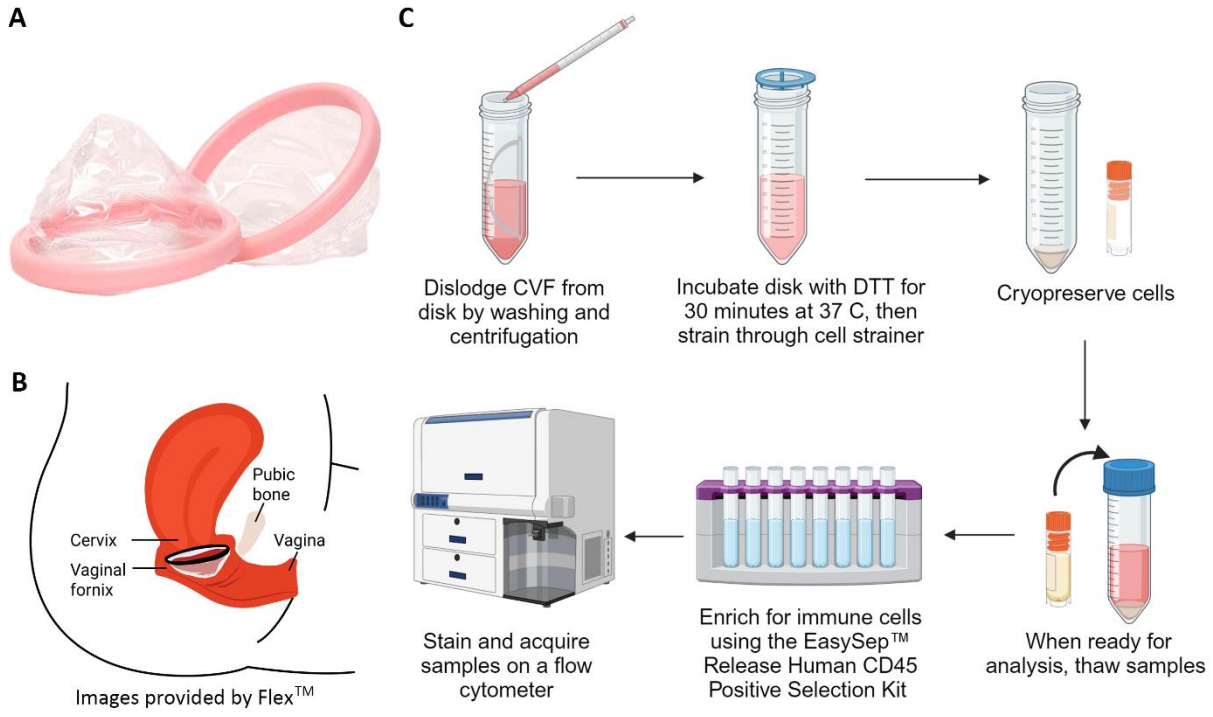

Figure 1. Menstrual disc sample collection and processing overview. (A) Softdisc® with firm plastic ring and soft plastic cup used to collect CVF. **(B)** Placement of the menstrual disc across the cervix and positioned to collect CVF. Images in panel A and B are subject to Copyright ©2023 The Flex Company, www.flexfits.com. All rights reserved. SOFTDISC is a registered trademark of The Flex Company. **(C)** Overview of method for processing and analyzing CVF for immune cells. Figure created with BioRender.com.

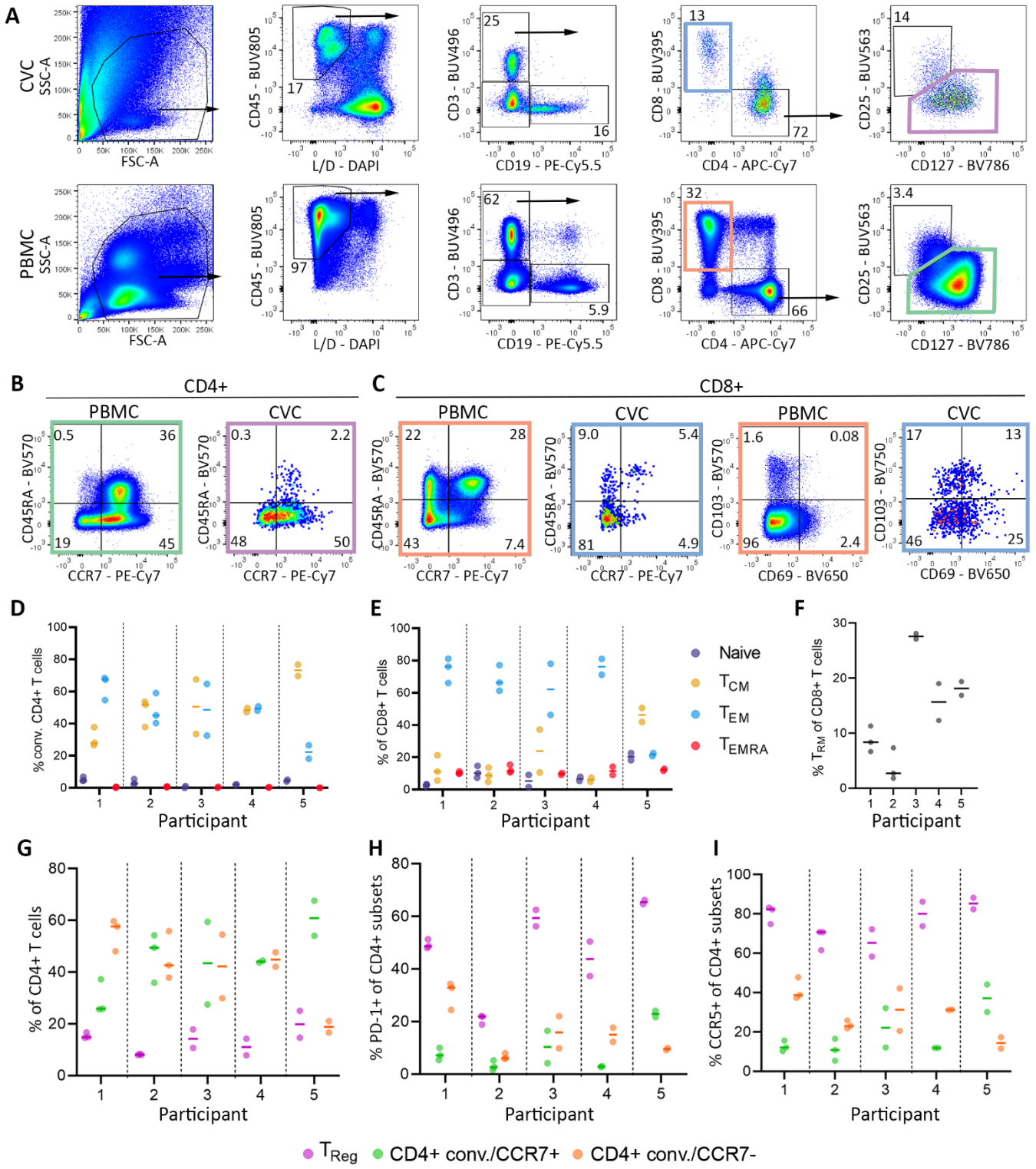

Figure 2. Overview of CVC T cell populations. Data from five individuals sampled across three days. Samples with greater than 50 cells in the parent population for each analysis represented in plots. (**A**) Representative gates for identification of T cells and other immune subpopulations in CVC (top) and

PBMC (bottom) samples. γδ-T cells and MAIT cells were excluded from the T cell population prior to gating into CD4 and CD8 subpopulations. (**B**) After gating out Tregs, conventional CD4+ T cells were further gated by CCR7 and CD45RA to define effector memory (T_{EM}), central memory (T_{CM}), terminally differentiated effector memory (T_{EMRA}), and naïve-like populations for PBMC (left) and CVC (right) samples. (**C**) CD8+ T cells were also gated by CCR7 and CD45RA to determine memory subtypes, as well as by CD69 and CD103 to determine tissue residency. (**D**) Frequency of conventional CVC CD4+ memory subtypes across samples. (**E**) Frequency of CVC CD8+ memory subtypes across samples. (**F**) Frequency of CVC CD8+ T_{RM} across samples. (**G**) Frequencies of CVC Tregs, conventional CCR7+, and conventional CCR7- cells of all CD4+ T cells. (**H**) PD-1 expression on CVC CD4+ T cells. (**I**) CCR5 expression on CVC CD4+ T cells.

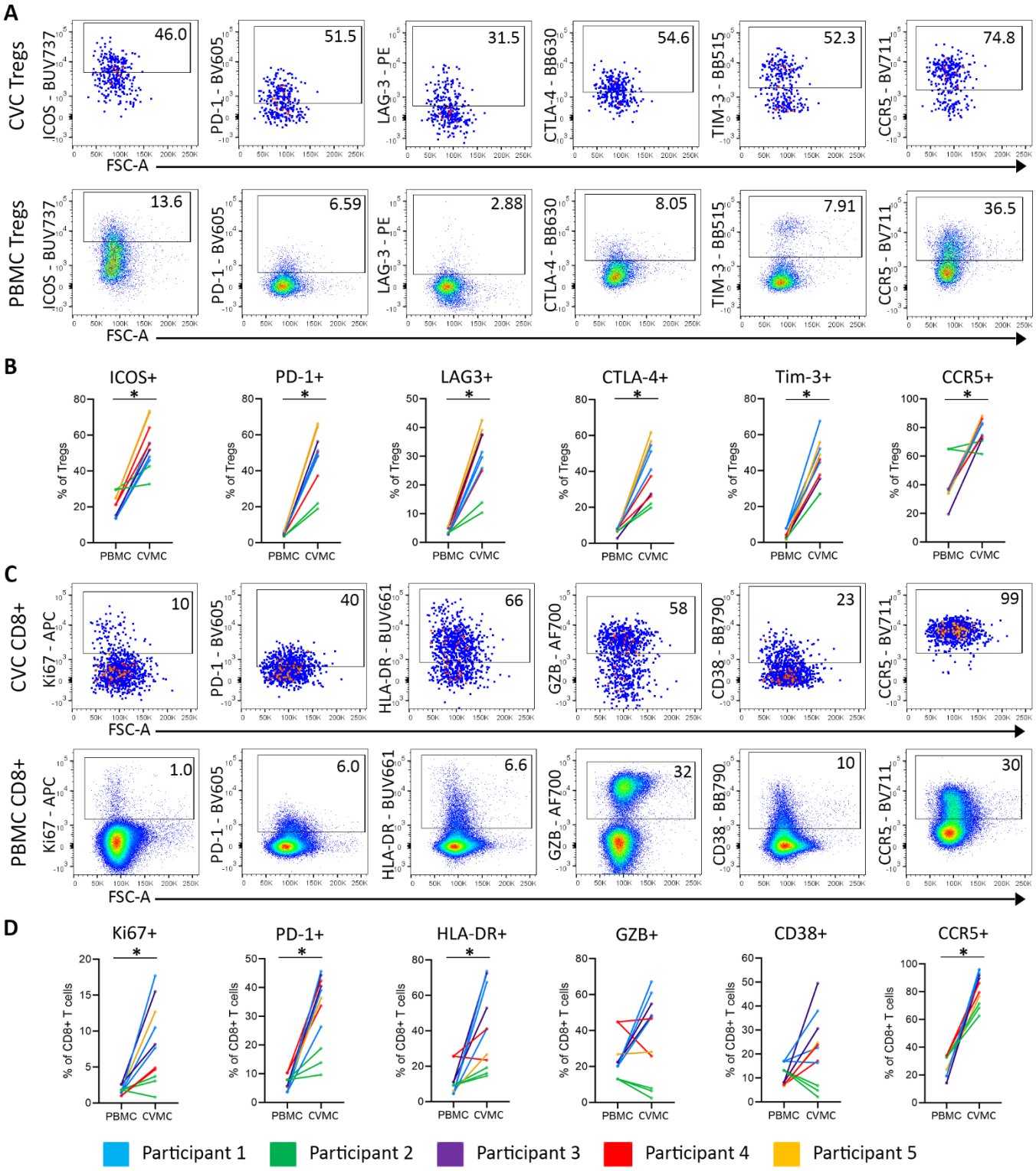

Figure 3. Characterization of key CVC T cell populations. Data from five individuals sampled across three (CVC) and one (PBMC) day. Samples with greater than 50 cells in the parent population for each analysis included. The mean CVC frequency of each population of interest across sampled days was

compared to the PBMC frequency using a Wilcoxon signed rank test. Star indicates p value less than or equal to 0.05. **(A)** Representative flow plots of activation and suppression marker expression from paired CVC and PBMC Treg populations. **(B)** Summary plots of frequencies of activation and suppression markers between paired CVC and PBMC Treg populations. **(C)** Representative flow plots of activation and suppression marker expression from paired CVC and PBMC memory CD8+ T cells. **(D)** Summary plots of frequencies of activation and suppression markers between paired CVC and PBMC memory CD8+ T cells.

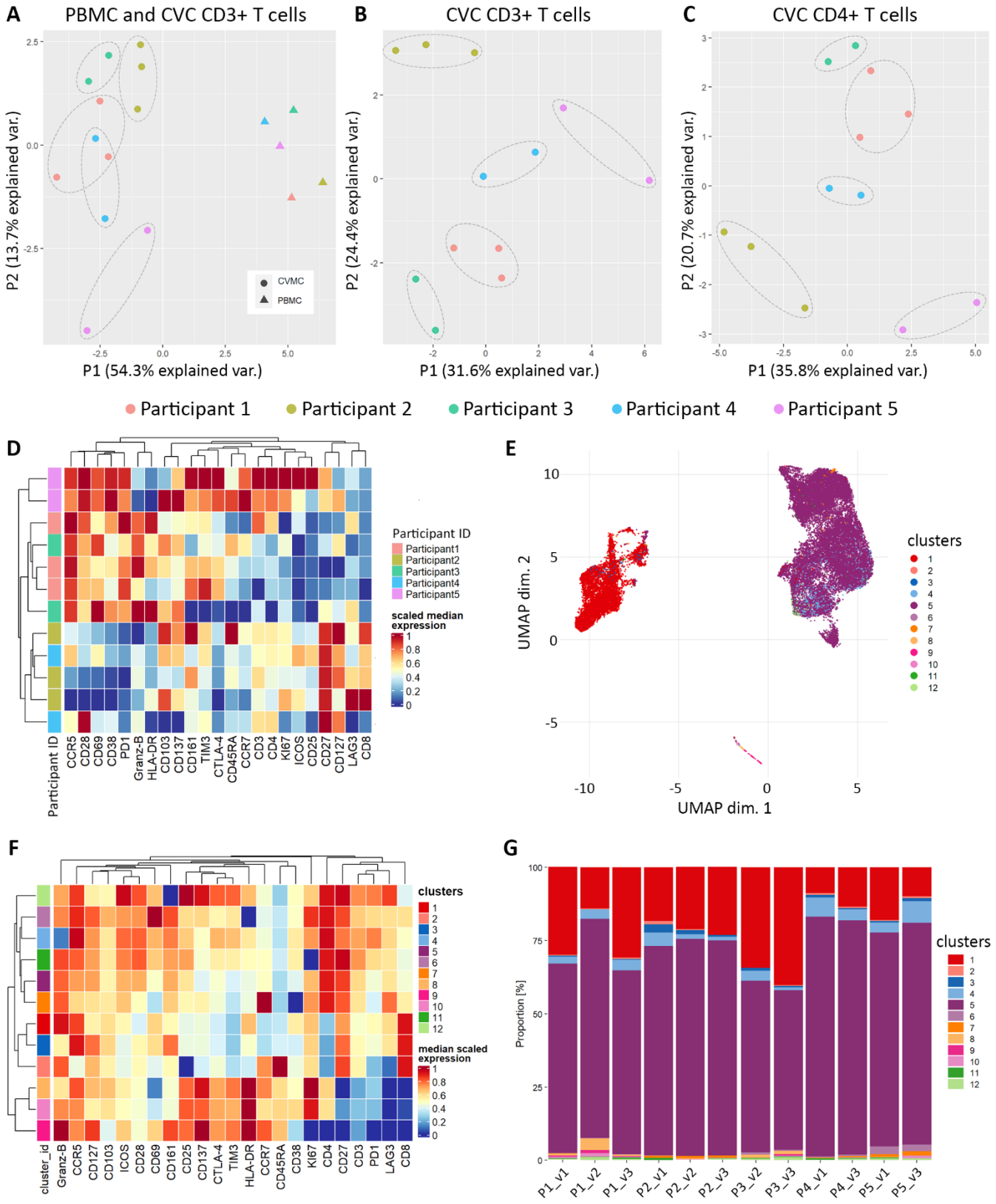
A
PBMC and CVC CD3+ T cells
P2 (13.7% explained var.)
P1 (54.3% explained var.)
CVMC
PBMC
B
CVC CD3+ T cells
P2 (24.4% explained var.)
P1 (31.6% explained var.)
C
CVC CD4+ T cells
P2 (20.7% explained var.)
P1 (35.8% explained var.)
Participant 1
Participant 2
Participant 3
Participant 4
Participant 5
D
Participant ID
Participant1
Participant2
Participant3
Participant4
Participant5
scaled median expression
CCR5 CD28 CD69 CD38 PD1 Granz-B HLA-DR CD103 CD137 CD161 TIM3 CTLA-4 CD45RA CCR7 CD3 CD4 KI67 ICOS CD25 CD27 CD127 LAG3 CD8
E
UMAP dim. 2
UMAP dim. 1
clusters
F
clusters
median scaled expression
cluster_id Granz-B CCR5 CD127 CD103 ICOS CD28 CD69 CD161 CD25 CD137 CTLA-4 TIM3 HLA-DR CCR7 CD45RA CD38 KI67 CD4 CD27 CD3 PD1 LAG3 CD8
G
Proportion [%]
clusters
P1_v1 P1_v2 P1_v3 P2_v1 P2_v2 P2_v3 P3_v2 P3_v3 P4_v1 P4_v3 P5_v1 P5_v3

526

Figure 4. CVC T cell populations are reproducible within individuals but vary across individuals. Data from five individuals sampled across three (CVC) and one (PBMC) day. Samples with greater than 100 cells in the parent population for each analysis included. **(A)** PCA utilizing high parameter flow data to characterize paired CVC and PBMC CD3+ T cell memory populations. **(B)** PCA characterizing CVC CD3+ memory T cell populations. **(C)** PCA characterizing CVC CD4+ T cell populations. **(D)** Unsupervised hierarchical heat map characterizing the median expression of CVC T cell markers across individuals and samples. **(E)** Dimensional reduction of all markers relevant to T cells was performed and is represented as a UMAP including all CD3+ T cells across CVC samples. **(F)** Heat map characterizing the median expression of T cell markers in each identified cluster. **(G)** Proportions of cell clusters composing each sample, arranged by participant and visit.